

ESTIMATION OF CARBON STOCKS IN NEW ZEALAND PLANTED FORESTS USING AIRBORNE SCANNING LIDAR

P.R. Stephens¹, P. J. Watt², D. Loubser¹, A. Haywood³, M.O. Kimberley⁴

¹ Ministry for the Environment, PO Box 10362, Wellington, New Zealand – (Peter.Stephens, David.Loubser)@mfe.govt.nz

² Pöyry Forest Industry, PO Box 105891, Auckland, New Zealand – pete.watt@poyry.com

³ Pöyry Forest Industry, Box 22, 437 St. Kilda Road, Melbourne, Australia – andrew.haywood@poyry.com

⁴ Forest Research Institute, Private Bag 3020, Rotorua, New Zealand – mark.kimberley@ensisjv.com

KEY WORDS: Kyoto Protocol, forest inventory, sampling, carbon models

ABSTRACT:

To meet obligations under Article 3.3 of the Kyoto Protocol, New Zealand is required to estimate, in an unbiased manner, forest carbon stock change, over the Protocol's first commitment period (2008-2012). New Zealand has three categories of forest, namely: natural forest; forests planted prior to 1990; and forests planted in non-forest land after 1990. Carbon credits can be earned from net carbon accumulated in the last forest category: these forests are referred to as 'Kyoto forests'. However, field access to these Kyoto forests for sampling is not guaranteed, and a plot-based forest carbon inventory system, which relies on the use of airborne scanning LiDAR, was therefore developed. Circular plots, 0.06 ha in area, will be located within these forests on a systematic 4 km grid. This paper describes investigations to confirm the relationship at the plot scale between LiDAR variables and (a) forest carbon, and (b) the key inputs (namely height, basal area, age, and silvicultural regime) to a New Zealand-specific forest growth model. The study has demonstrated that airborne scanning LiDAR provides an alternative approach to estimate carbon stock change for the first commitment period of the Kyoto Protocol, and can provide inputs to forest growth and carbon models enabling forecasts of carbon sequestration beyond 2012. The paper also describes some considerations for an operational forest carbon inventory system which will be implemented in early 2008.

1. INTRODUCTION

New Zealand is a signatory to the Kyoto Protocol and the United Nations Framework Convention on Climate Change. A requirement under Article 3.3 of the Protocol is annual reporting of carbon stock changes arising from land use, land-use change and forestry (LULUCF) activities. Reporting is required for the Protocol's first commitment period, from 2008 to 2012. Good Practice Guidance for LULUCF activities requires carbon stock changes to be estimated in an unbiased, transparent, and consistent manner. Further, uncertainties must be determined and these are required to be reduced over time.

To meet LULUCF reporting requirements, New Zealand will be classifying forests into three categories: natural forest; forests planted prior to 1990; and forests planted after 1990 into non-forest land. The latter category is referred to as 'Kyoto forests'. Forests to be measured by New Zealand under the Protocol have been selected by the following parameters: minimum area of 1 ha; at least 30 % canopy cover; at least 5 m in height; and a width of 30 m. Carbon credits (net carbon stock change) derived from Kyoto forests over the first commitment period can then be used to either offset greenhouse gas emissions and/or for carbon trading. New Zealand planted forests are comprised predominantly (89 %) of radiata pine (*Pinus radiata*), with the remainder made up of other species, mostly (6 %) Douglas-fir (*Pseudotsuga menziesii*) (MAF, 2006).

A plot-based forest inventory system has been developed for Kyoto forests. Circular plots, 0.06 ha in area, will be located within these forests on a systematic 4 km grid across New Zealand. Field access to the mostly privately-owned Kyoto forests is not guaranteed. Accordingly, airborne scanning Light Detection and Ranging (LiDAR) will be used to inventory those

plots without field access. Plot measurements are then used as inputs to a New Zealand specific radiata pine growth model, the 300 Index (Kimberley et al., 2005) and a carbon allocation model, called C_Change (Beets et al., 1999). These two models can be linked, with the growth model used to parameterise the carbon allocation model. Under the Kyoto Protocol the four biomass carbon pools that must be reported are aboveground biomass, belowground biomass, dead wood, and litter. The amount of carbon in each of the four biomass carbon pools, at any stage of tree growth and stand development, is determined by running these two linked models.

In recent years researchers have published a wide range of methods using remotely-sensed data to help identify forest type and forest structure. Much of this work has been focused on mapping at a small scale using satellite imagery. New digital metric cameras and airborne LiDAR scanning instruments allow forest information to be measured in three dimensions with precision over moderately large areas at low unit cost. In some countries the data derived from digital airborne surveys and/or scanning LiDAR are being used (Næsset, 2002; Holmgren and Wallerman, 2006).

Airborne LiDAR has been studied for its application in forestry since 1978. However, it is only in recent years that the combination of global positioning systems (GPS), inertial navigation systems and improvements in post-processing capabilities have allowed the scanning LiDAR and digital camera technology to progress to operational use (Næsset, 2002; Nilsson, 1996; Watt, 2005).

This study was undertaken to determine the potential of airborne scanning LiDAR to determine forest characteristics at

the plot scale (Watt and Haywood, 2007a). The criteria used to test the potential of airborne scanning LiDAR included accuracy with which the key inputs to the 300 Index growth model could be determined, and the accuracy of predicting total carbon at the inventory plot scale. The key inputs to this growth model include: mean top height; basal area; tree age; and silvicultural regime (stocking (trees per ha), pruning, and thinning). Mean top height is the mean height of the 100 largest diameter stems per ha, and its method of calculation is described by Dunlop (1995). Mean top height is derived from plot tree total heights and stem diameters measured in the field.

2. MATERIALS

2.1 Study Area

The study was located in the central area of the North Island, New Zealand (39° S, 176° E) and consisted of both planted forest inventory plots and experimental trial plots for which we had unrestricted field access. Field and LiDAR data were collected between August and October 2006. The forests in these plots were representative of the radiata pine dominated forests in New Zealand.

2.2 Field Plot Data and Carbon Stocks

To determine how well LiDAR could predict inputs to the growth model, 121 plots were used ranging in size from 0.04 to 0.245 ha, and arrangement: circular, square and/or rectangular. The circular plots had been measured in 4 plot clusters (a central plot with three satellite plots within 35 m of the central plot), while the square and rectangular plots were generally measured as part of existing experiments. Measurements recorded for each plot included: age; stocking; tree diameter at breast height; tree heights; and pruned height. Radiata pine plantations occurred in 117 of these plots. A summary of the field measurements and statistics is provided in Table 1.

Field plot centres were located using a 12-channel differential GPS. The positional accuracy of the survey is expected to be within ± 3 m. In a majority of plots individual tree locations were also recorded in relation to the plot centre.

	Mean	SD	Median	Min	Max
Top Height (m)	22.9	8.6	22.7	2.8	39.1
Basal Area (m ² /ha)	33.3	13.6	35.9	0.4	62.0
Stocking (trees/ha)	468	446	468	81	4435
Age (years)	16.1	5.5	19	4	26

Table 1. Summary of plot statistics ($n=121$).

To determine the accuracy of LiDAR variables to predict total carbon per plot, 140 plots were used. Thirty six Kyoto forest radiata pine plantation plots with a pasture land-use history were added to the original (121) plot set, and 17 of the original plots, comprised of very young trees, were excluded. The total carbon for each of the 140 plots was determined by using field measured and derived inputs to the 300 Index growth model. The mean total carbon for the 140 plots was 117 t/ha, with a range from 36 - 261 t/ha.

2.3 LiDAR and Photographic Data

The LiDAR data were acquired using a small footprint (0.2 m) Optech ALTM 3100EA system at 8-10 returns/m². The 3100EA system is capable of recording the return time of up to four pulses, the first is usually reflected from the top of the canopy and intermediate pulses from the lower canopy or ground. Aerial photographic data were captured, for reference only, using a natural colour Rollei AIC medium format digital camera. These data had a pixel size corresponding to 20 cm on the ground.

3. METHODS

3.1 LiDAR Data Analysis

The analysis of the LiDAR data involved a five-stage process, as listed below.

1. Calculation of LiDAR plot-level variables, such as height percentiles and coefficient of variation of above ground pulse responses. LiDAR data were also used to determine ground height within the plots.
2. Exploratory analysis of the two datasets - field measurements and LiDAR data - to investigate their underlying data structure.
3. Generation, using bivariate and multiple regression methods, of relationships at plot level between field measurements (mean top height, stocking, and basal area) and total carbon per plot to LiDAR-derived variables.
4. Determination of stocking using an individual tree detection method.
5. Progressive decimation of the number of LiDAR returns on the ability of LiDAR to predict top height and basal area at the plot level.

3.2 Variables Derived from LiDAR Data

The following variables were calculated from the LiDAR data and extracted over co-located field plots for quantitative analysis: LiDAR height percentiles; mean intensity percentiles; standard deviation of laser dispersals; percentage of ground returns; coefficient of variation; skewness and kurtosis.

LiDAR height percentiles provide information on the structure of the forest canopy at different height levels. Using the LiDAR data the pulses above 0.5 m were divided into quantiles corresponding to every 10th percentile from the 10th to the 100th, as well as the 5th, 95th and 99th percentiles. The 0.5 m was used as a threshold to account for undulations in terrain. This provided 13 variables of an average LiDAR canopy height by percentile.

Laser intensity, the intensity of each return pulse (sometimes referred to as laser amplitude), represents this reflected energy and provides a concentrated measurement of the object's reflectance unaffected by shadows or occlusions. This reflectance may vary based on the reflectance properties and porosity of the targeted material, path length and incidence angle of the pulse. Accordingly, for this study the data are regarded as uncalibrated, and is only used as a relative measure of intensity. For each plot the mean intensity for each of the 13 height percentiles was calculated.

The standard deviation of laser dispersals provides a simple measurement of the variation or dispersal within the laser height distribution of each field measurement plot.

The percentage of ground returns (*pczero*) provides a measure of canopy density, and is calculated by dividing the sum of all above ground returns by ground observations with height values below 0.5 m by the total number of returns. All returns above this threshold are considered to be canopy hits. Areas with large numbers of ground returns will be those with sparser, more open canopies.

The coefficient of variation (C_V) summarises the relative variation, or dispersion, of the LiDAR height distribution within each sample plot. It is the ratio of standard deviation and mean, and is expressed as a percentage. As a measure of crown density, higher C_V values indicate sparse, open canopies and low C_V values dense, closed canopies (e.g. <20%). The inclusion of C_V has proven useful to other researchers for estimating basal area, volume and biomass (Næsset, 1997; Nelson et al., 1997; Næsset & Økland, 2002).

Skewness (*skew*) and kurtosis (*kurt*) of LiDAR height distribution also provide measures of canopy structure and density. If returns from the forest canopy only are considered, then as trees increase in height and the canopy develops, skewness and kurtosis of the laser height distribution change.

3.3 Exploratory Data Analysis

This analysis was used to explore, organise and summarise patterns in the LiDAR data, to explain variation and strength of relationships between the LiDAR-derived variables. Firstly, computation of summary statistics (Table 1) and the exploration of the distributional properties of all variables using histograms was undertaken. This was important to both detect and remove errors in the dataset and to identify factors such as outliers (due to uncertainty in location of field plots) that may potentially influence any modelling. Secondly, the correlation between each variable within the datasets was calculated as an initial step to the identification of potential relationships.

3.4 Regression Modelling

Regression equations were fitted to predict five forest structural variables, namely: top height; basal area; stocking; age; and total carbon. LiDAR data from the 117 radiata pine plots were used to calculate the predictor variables in these regression equations. Eight types of predictor variables were used in this analysis. These are: mean LiDAR height by height percentile; mean intensity by height percentile; standard deviation of LiDAR dispersion; percentage of ground returns (*pczero*); reciprocal of *pczero* (*pcveg*); coefficient of variation (C_V); skewness (*skew*); and kurtosis (*kurt*).

Two regression modelling approaches were used given the relationships between the datasets. These approaches were bivariate (for top height) and multiple regression (for basal area, stocking, age, and total carbon).

Bivariate regression uses the different LiDAR derived data individually as predictor variables for the estimation of the structural parameters. For each variable, the laser height percentile with the highest R^2 and lowest residual mean square (RMS) error values was used. Selection was guided first by the R^2 and then RMS values. This approach was only applied to top height, as previous studies showed that although bivariate regression worked well with top height, it would not be sufficient for the estimation of the other forest structural parameters (Donoghue and Watt, 2006; Watt and Haywood, 2006).

Multiple regression analysis was conducted to determine if further variation in the models could be explained by the inclusion of LiDAR-derived measures of intensity and canopy structure/density.

3.5 Progressive decimation of LiDAR returns

To test the sensitivity of the relationships to changes in LiDAR point density, returns classed as vegetation and ground data surrounding the plots were progressively decimated (reduced in number) using a randomised sampling routine (Watt and Haywood, 2007b). A ground surface model was generated for the area around each plot cluster for each iteration. It is necessary to process an area larger than the plot extent to ensure that there are an adequate number of LiDAR ground returns to generate the ground surface model. Using the surface model as a reference, relative height of each LiDAR return above the ground was calculated for the area in and surrounding the plot.

The impact of progressively reducing the number of laser returns on regression model error was tested using tenfold cross-validation. In tenfold cross validation each dataset is divided into 10 subsets of approximately equal size; the model is re-run 10 times, each time leaving out one of the subsets and utilising it for testing the model. The sample error is then calculated each time and averaged to obtain an estimate of the true error. For each run the 'optimal model' was selected measured in terms of the model with the lowest RMS error.

3.6 Automatic Tree Detection

An individual tree detection algorithm was also used as a method for determining tree stocking. The algorithm uses canopy returns to detect individual tree crowns, and is based on the work conducted by Holmgren and Wallerman (2006). The algorithm was evaluated over 10 stands with the accuracy of the detection compared plot-level stocking.

4. RESULTS

4.1 Top Height Prediction Using LiDAR Percentiles

The percentile height with highest R^2 and lowest RMS error was selected as the predictor for estimation of top height. In this case, laser height values corresponding to the 70th percentile (*p70*) were used. Figure 1 illustrates there is a strong linear relationship ($R^2 = 0.96$) between the 70th height percentile (*p70*) and field-measured top height.

With an R^2 of 0.96 using a single variable it is clear that a simple model that uses a single height percentile is the most effective approach to a prediction of top height. Canopy density variables did not add any additional value to the predictive model in terms of explaining the remaining variation.

4.2 Basal Area Prediction Using LiDAR Data

Multiple regression showed that none of the intensity measurements were significant (with $p > 0.05$). Accordingly, the 30th height percentile (*p30*) measurement and skewness (*skew*) were the only variables included in the model. This model had an R^2 of 0.66 with an RMS error of 8.02 m² (25%). Figure 2 shows the relationship between basal area and the two significant variables (*p30* and *skew*). The 30th height percentile

is positively correlated with basal area, while skewness is negatively correlated.

Figure 2 shows that there are no strong outliers in the dataset causing undue influence on the regression. There are no major patterns or structure in the residuals, which indicates that the model predicts basal area reasonably well at both high and low basal area.

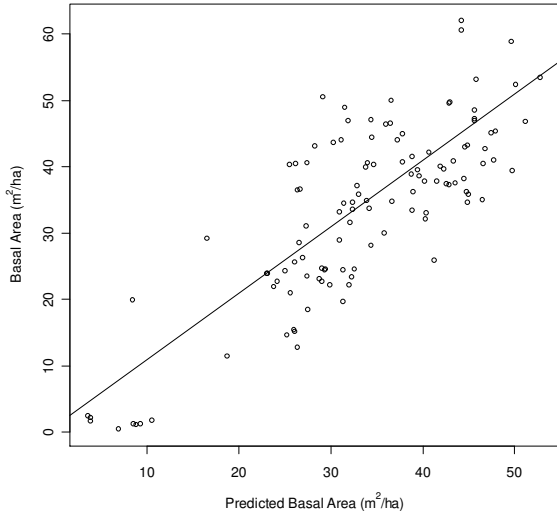


Figure 1. Top height against LiDAR 70th height percentile (*p70*) ($n=117$).

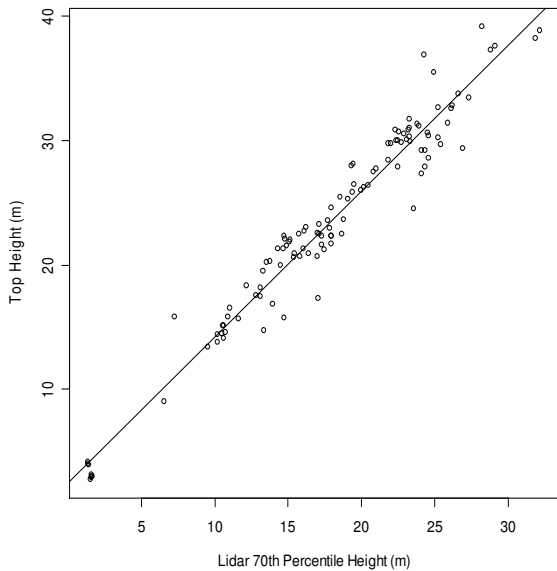


Figure 2. LiDAR-derived basal area against field measured basal area ($n=117$).

4.3 Stocking (Stems per ha)

Multiple regression analysis showed that the only models found to be significant were models with a single height percentile measurement. The model with the highest R^2 and lowest RMS error was the model that included maximum height (*p100*). The stocking model based on the highest R^2 ($R^2 = 0.26$ and RMS error = 167 stems/ha (35%)) does not provide a good relationship. There are no strong outliers in the dataset causing

undue influence on the regression. The RMS error is high, limiting its practical use for providing stocking estimates.

4.4 Tree Age Prediction Using LiDAR Percentiles

The best model for predicting age included both height and a canopy structural measure. A model that includes height (*p60*) and kurtosis (*kurt*), explained 74% of the variation with an RMS error of 2.85 years (18%).

4.5 Total Carbon Per Plot Using LiDAR Data

Bivariate regression showed that there was a strong relationship between modelled total carbon per plot and tree height. A single LiDAR canopy height percentile (*p30*) explained 71 % of the variation in modelled total carbon. When combined with canopy structure (*pczero*) there was a significant improvement with fit, with 80 % variance explained (Figure 3). It was established that if a robust measure of stocking were available for LiDAR, then 87% of the variation in modelled total carbon could be explained.

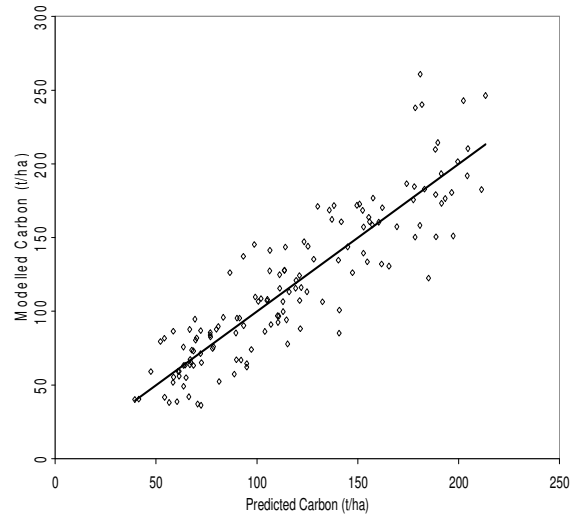


Figure 3. Modelled versus predicted carbon using LiDAR-derived inputs to the 300 Index growth model and the C_Change carbon allocation model ($n=140$).

4.6 Decimation of LiDAR Returns

Top height and basal area relationships behaved in a similar manner with the decimation model structure, remaining relatively stable throughout all runs. As expected the RMS error tends to increase as laser point density decreases with the greatest observed once densities fall below 1%, a nominal point density of 0.1 returns/m². At densities below this the models start to perform poorly.

4.7 Stocking Estimates From Automatic Tree Detection

The ability of the algorithm to detect trees depends on the laser return density, crown size, tree height and growth stage. The RMS error of the non-linear least square regression is 140 stems/ha. Overall the algorithm underestimated the number of trees, with larger errors observed in plots that contain higher numbers of trees. The proportion of detected trees saturates once stocking levels exceed 1200 stems/ha.

5. DISCUSSION

This study sought to determine the potential benefit of airborne scanning LiDAR as an input to carbon models and to estimate carbon per plot for New Zealand Kyoto forests. It is anticipated that some of the methods described in this paper will become operational and that LiDAR data will be used routinely to provide plot-based estimates of carbon as well as some key carbon model parameters. Based on work reported here, we have demonstrated that LiDAR is able to provide estimates of total carbon per plot ($R^2=0.80$), mean top height ($R^2=0.96$), basal area ($R^2=0.66$), and age ($R^2=0.74$). The following discussion compares this research against an earlier South Island study in New Zealand (Watt and Haywood, 2006) and also attempts to place the results in a wider international context.

Total carbon per plot could be predicted with a reasonable level of precision ($R^2=0.80$; RMS error = 23 t (carbon) per ha (19%)), where LiDAR derived height at the 30th percentile ($p30$) has an $R^2 = 0.71$. Predictive performance was improved by including stocking in the regression model ($R^2=0.87$; RMS error = 19 t (carbon) per ha (16%)). These results were superior to results from the earlier South Island study (Watt and Haywood, 2006), where the regression model with three LiDAR variables had an $R^2=0.59$ and an RMS error = 24 t (carbon) per ha (37%). This inferior result is likely to be due to difficulties in precisely matching ground and LiDAR plot locations, and a result of the time of LiDAR data acquisition being up to 1.5 years after the plot measurements were made for the 74 plots.

In this study a strong relationship ($R^2 = 0.96$; RMS error = 1.82 m (8%)) between mean top height and LiDAR derived heights above the 70th percentile ($p70$) was established. This result is similar to that obtained in the earlier New Zealand study (Watt and Haywood, 2006) which yielded R^2 values of ≥ 0.87 with an RMS error of ≤ 1.36 m. Again, the results from the Watt and Haywood (2006) study suggest that the linear model is relatively insensitive to LiDAR height distribution percentiles above 60%. Combined, these results agree with international findings where the accuracy of LiDAR-derived height is comparable to that of manual field survey methods (Donoghue and Watt, 2006; Næsset, 1997; Watt, 2005; Lim and Treitz, 2004). To achieve a good level of accuracy the density of laser returns must be sufficient to (a) define the underlying terrain and (b) capture variations in terms of tree crop height and spatial arrangement. Generally a survey that records at least 1 to 2 first returns/m² at a scan angle of $\leq 10^\circ$ either side of nadir should be sufficient to capture the detail required (Watt, 2005; Watt and Haywood, 2007b).

Basal area estimates based on LiDAR measurements were found to be less accurate than top height; the best model found had an R^2 of 0.66 with an RMS error of 8.02 m² (25%). The error found in this study is of a similar magnitude to that found in the earlier New Zealand study (Watt and Haywood, 2006). The field-measured basal area was found to be strongly correlated with top height ($R^2 = 0.73$). The final model included height ($p30$) and skewness. The height measure can be interpreted as being a measure of the development phase of the plot which is related directly to basal area. In European conifer-dominated forest Næsset (2002) reported R^2 values of 0.86 for basal area in southern Norway, and Lim et al. (2003) reported basal area estimates of $R^2=0.86$ in a Canadian hardwood forest.

Stocking was not reliably predicted using LiDAR measurements in this study. The RMS error is high (167 stems/ha (35%)) limiting its practical use for providing accurate estimates of tree

density. This result is in contrast to other studies where the inclusion of measures of canopy characteristics derived from the LiDAR height distribution, in combination with selected LiDAR height percentiles, have proven useful for estimating stocking (Næsset, 2002). One explanation is that after stocking has changed (a standard silvicultural treatment) in New Zealand conifer forests the tree crowns expand to fill the canopy gaps and so while the stocking may change the distribution of LiDAR points may be similar to areas that have received no treatment once the canopy has closed.

The evaluation of the single tree detection algorithm shows that the RMS error is marginally lower than the plot-based method. Overall the algorithm provides better results in stands less than 1200 stems/ha. Above this stocking level the method saturated, especially in areas with coalescing crowns. To measure higher density stands it would be necessary to sharpen the tree top extraction algorithm. The detection rate would probably also improve if a higher density laser dataset was used. However, according to the simulations, the detection rate would still decrease as a function of stem density even if a high density laser dataset (20 returns/m²) were available. Therefore, it would be necessary to have a method for the estimation of the number of sub-dominant or suppressed trees.

Estimates of age were improved by including more than just LiDAR-derived height. A model that includes height ($p60$) and kurtosis (*kurt*) explains 74% of the variation with RMS error of 2.85 years (18%). Here, kurtosis provides a measure of canopy permeability which is related to tree crop development stage. Both variables included in the model are uncorrelated, so assist in explaining variation associated with the prediction.

Any reduction in the point density (number of pulses/m²) of a LiDAR survey has the potential to reduce acquisition costs of data. This study evaluated for basal area and top height the effect of systematically reducing the laser point density and showed that basal area and top height estimates are stable even after 95% of the original data has been removed. This is equivalent to reducing the initial point density of 9 returns/m² to 0.5 returns/m². A plausible explanation is the simple structure of top height and basal area models, as for both, height percentiles are the most significant variables. Consequently, the models are relatively insensitive to the decimation process. These findings are similar to other research that has evaluated different laser point densities and their impact on plot-level forest predictions (Næsset, 2002; Goodwin et al., 2006). Also of relevance to this work is that little change is observed in predictions if pulse density is kept constant and footprint size (0.2 to 0.6 m) and platform altitude are increased (Næsset, 2002; Goodwin et al., 2006).

While silvicultural status was not assessed in this study, an earlier study in New Zealand (Watt and Haywood, 2006) noted that for Kyoto forest plots, prune heights can be determined by visual assessment of LiDAR data. If automatic methods do not show promise in determining this aspect of management, then visual methods could be employed.

6. CONCLUSIONS

Where field access to forest plots is not possible, the study has demonstrated that airborne scanning LiDAR provides an alternative operational approach to estimate, at the plot-level, total carbon change for the first commitment period of the Kyoto Protocol. Forest top height, basal area, and age can be

determined with acceptable accuracy. It is expected that either visual assessment of either digital photography and/or LiDAR data can address the stocking (stems per ha) issue.

This study suggests that laser point density can be taken as low as 0.5 to 1 returns/m² without unduly affecting predictions of basal area and top height. Assessment of stocking using laser returns will require a much higher density. Given there will be variation in the number of returns across a survey area (in the study the range was 3-19 returns/m² due to overlapping LiDAR swaths), it is prudent to acquire data at more than 4 returns/m². This should provide a margin of safety and reduce the possibility of plots being excluded from the analysis due to insufficient laser returns, and to support use of LiDAR data to assess stocking should visual assessment of photographic imagery not be possible.

The ability of LiDAR to provide inputs to the linked forest growth and carbon models with some degree of accuracy will assist in forecasting carbon sequestration beyond 2012.

Operationally, adequate measurements to estimate carbon stock change for the first commitment period of the Kyoto Protocol could be achieved by surveying the Kyoto forest plot network located on a 4 km grid in 2008 and in 2012. The Kyoto forest plots will be circular, and 0.06 ha in area. During this five year period, as more data are acquired, the regression relationship between LiDAR variables and carbon per plot will be reviewed and improved. This will enable more accurate relationships to be applied to past plot data, which subsequently will lead to updated carbon assessments and a reduction in uncertainties, as is required under the Kyoto Protocol.

7. REFERENCES

- Beets, P.N., Robertson, K.A., Ford-Robertson, J.B., Gordon, J., and Maclaren, J.P., 1999. Description and validation of C_Change: A model for simulating carbon content in managed *Pinus Radiata* stands. *New Zealand Journal of Forestry Science*, 29(3), pp. 409-427.
- Donoghue, D.N.M., and Watt, P.J., 2006. Using LiDAR to compare forest height estimates from IKONOS and Landsat ETM+ data in Sitka spruce plantation forests. *International Journal of Remote Sensing*, 27(11), pp. 2161-2175.
- Dunlop, J., 1995. Permanent sample plot system User Manual. New Zealand Forest Research Institute Bulletin No. 187, Rotorua, New Zealand.
- Kimberly, M.O., West, G.G., Dean, M.G., Knowles, L.R., 2005. The 300 Index – a volume productivity index for radiata pine. *New Zealand Journal of Forestry*, 50, pp. 13-18.
- Lim, K., Treitz, P., Wulder, M., St-Onge, B., Flood, M., 2003. LiDAR remote sensing of forest structure. *Progress In Physical Geography*, 27(1), pp. 88-106.
- Lim, K.S., and Treitz, P.M., 2004. Estimation of above ground forest biomass from airborne discrete return laser scanner data using canopy-based quantile estimators. *Scandinavian Journal of Forest Research*, 19(6), pp. 558-570.
- Goodwin, N. R., Coops, N.C., Culvenor, D.S., 2006. Assessment of forest structure with airborne LiDAR and the effects of platform altitude. *Remote Sensing of Environment*, 103(2), pp. 140-152.
- Holmgren, J., and Wallerman, J., 2006. Estimation of tree size distribution by combining vertical and horizontal distribution of LiDAR measurements with extraction of individual trees. In: *Proceedings, EARSeL ISPRS Workshop, 3D Remote Sensing in Forestry*, Vienna, pp. 157-163.
- Næsset, E., 1997. Estimating timber volume of forest stands using airborne laser scanner data. *Remote Sensing of Environment*, 61(2), pp.246-253.
- Næsset, E., and Økland, T., 2002. Estimating tree height and tree crown properties using airborne scanning laser in a boreal nature reserve. *Remote Sensing of Environment*, 79(1), pp. 105-115.
- MAF, 2006: A National Exotic Forest Description as at 1 April 2005. Edition 22, Ministry of Agriculture and Forestry, Wellington, New Zealand.
- Næsset, E., 2002. Predicting forest stand characteristics with airborne laser using a practical two-stage procedure and field data. *Remote Sensing of Environment*, 80, pp. 88–99.
- Nelson, R., Oderwald, R., Gregoire, T.G., 1997. Separating the ground and airborne laser sampling phases to estimate tropical forest basal area, volume, and biomass. *Remote Sensing of Environment*, 60(3), pp. 311-326.
- Nilsson, M., 1996. Estimation of tree heights and stand volume using an airborne lidar system. *Remote Sensing of Environment*, 56, pp. 1–7.
- Watt, P.J., 2005. An evaluation of LiDAR and optical satellite data for the measurement of structural attributes in British upland conifer plantation forestry. Doctoral thesis. Department of Geography, University of Durham, England.
- Watt, P.J., and Haywood, A., 2006. Evaluation of airborne scanning LiDAR generated data as input into biomass/carbon models. Pöry Forest Industry, contract report 38A08068 to Ministry for the Environment, Wellington, New Zealand.
- Watt, P.J., and Haywood, A., 2007a. Evaluation of airborne scanning LiDAR generated data as input into biomass/carbon models. Pöry Forest Industry, contract report 38A07375 to Ministry for the Environment, Wellington, New Zealand.
- Watt, P.J., and Haywood, A., 2007b. Evaluation of the impact of varying LiDAR point density on the accuracy of LiDAR-derived forest estimation models. Pöry Forest Industry, contract report 38A08467 to Ministry for the Environment, Wellington, New Zealand.